

# Semantically Grounded QFormer for Efficient Vision Language Understanding

Moulik Choraria\*

University of Illinois at Urbana Champaign  
moulikc2@illinois.edu

Sourya Basu

University of Illinois at Urbana Champaign  
sourya@illinois.edu

Xu Zhang  
Amazon

xzhnamz@amazon.com

Prateek Singhal  
Amazon

prtksngh@amazon.com

Xinbo Wu\*

University of Illinois at Urbana Champaign  
xinbowu2@illinois.edu

Nitesh Sekhar  
Amazon

seknites@amazon.com

Yue Wu  
Amazon

wuayue@amazon.com

Lav R. Varshney

University of Illinois at Urbana Champaign  
varshney@illinois.edu

## Abstract

*General purpose Vision Language Models (VLMs) have received tremendous interest in recent years, owing to their ability to learn rich vision-language correlations as well as their broad zero-shot competencies. One immensely popular line of work utilizes frozen unimodal models, by bridging vision representations to language using a trainable module called the QFormer. However, this method relies heavily on large-scale multimodal pretraining with huge computational overheads. To that end, we propose a more efficient framework for QFormer-based vision-language alignment. Our key idea relies on the observation that QFormer latents correspond more strongly to the frozen LLM’s intermediate latent space. Consequently, instead of using QFormer latents as inputs to the LLM, we alter the framework by using the latents to directly condition the LLM latent space for image-to-text generation. We demonstrate the effectiveness of our approach against existing baselines in improving the efficiency of vision-language pretraining.*

## 1. Introduction

Vision-language models (VLMs) are a rapidly emerging topic of research due to their ability to harness multi-modal inputs for simultaneous visual and textual comprehension for diverse applications. Following the success of general purpose large language models [1, 3], efforts are underway towards analogous general purpose VLMs with few-shot learning capabilities. As such, methods relying on instruction finetuning [26, 27] are appealing due to their ability to

exploit natural language understanding; one particular line of work that combines it with multi-modal fusion of frozen language and vision models has received tremendous attention [5, 12]. Specifically, [12] relies on combining frozen unimodal representations via a multi-stage pretrained QFormer, followed by multi-task instruction finetuning, yielding state-of-the-art zero-shot performance on a variety of tasks [5]. Following their success, a slew of recent methods explore alternate strategies, while building on top of the QFormer base [13, 31].

The success of [12] heavily relies on the large-scale two-stage pretraining on the QFormer. In the first stage, the QFormer (initialized as a BERT model) is trained by a combination of self-supervised losses to learn a joint representation space (called Queries). In the next pretraining stage, the output Queries of the QFormer are fed to the frozen LLM to act as conditioning for end-to-end image-to-text generation. Ablation studies demonstrate that the two-stage large-scale pretraining plays a critical role in empowering the QFormer.

Despite the undeniable benefits however, the amount of data and compute required for pretraining at scale presents a very expensive hurdle, and remains inaccessible to the larger research community [21, 24]. In addition, curating diverse and unbiased multi-modal datasets requires substantial efforts to ensure VLMs do not inadvertently propagate harmful biases in the training data [30]. Hence, there is a pressing need for more efficient strategies for training VLMs and to that end, we seek to improve the pipeline in [5, 12].

Our contributions are as follows: we first analyze the QFormer representations, and its ease of modelling inputs for LLM conditioning. Specifically, we show that

\*These authors contributed equally to this work

the QFormer representations are better suited to model the frozen LLM’s intermediate representations. **Besides, we study existing alignment between different layers of language models and vision models.** Based on these insights, we propose an efficient alternative pipeline for QFormer-based vision-language modelling. Under controlled settings, we then demonstrate the effectiveness of our approach in both speeding up vision-language representation learning as well as improving performance.

## 2. Proposed Method

### 2.1. Problem Formulation

In this paper, we focus on the problem of training a general-purpose VLM, from the lens of instruction tuning. Specifically, given an image  $i$  and a text instruction/prompt  $p$ , the model should output an appropriate response corresponding to the inputs. Some example tasks include visual question answering where  $p$  is a question based on the image, or image captioning where  $p$  refers to the instruction of captioning the image. Within vision-language modelling, we focus on the QFormer-based line of work, that bridges frozen unimodal models via a smaller model (the QFormer [5, 11, 12]) for effective vision-language learning.

### 2.2. Revisiting InstructBLIP

InstructBLIP is one of the pioneering works on vision-language instruction tuning, utilizing the QFormer approach as a trainable bridge between frozen vision and language models. We first consider LLMs with encoder-decoder architectures [3, 6]. Then, the full InstructBLIP framework can be interpreted as four different modules.

**Image Encoder**  $\{v(\cdot)\}$ : This module extracts visual features from the image input  $i$ , using a frozen pretrained vision model.

**QFormer**  $\{Q(\cdot, \cdot, \cdot)\}$ : The QFormer takes in a set of learnable query tokens ( $\mathbf{t}_q$ ), the prompt  $p$ , and the encoder vision features  $v(i)$  and outputs visually informed query tokens  $\mathbf{t}_{qv}$ .

**LLM (Encoder-Decoder)**  $\{l_e([\cdot, \cdot]), l_d(\cdot)\}$ : The encoder takes the concatenation ( $[\cdot, \cdot]$  denotes concatenation) of the QFormer output tokens  $\mathbf{t}_{qv} = Q(\mathbf{t}_q, v(i), p)$  and the language prompt  $p$  as input and outputs a latent encoding, which is then used by the decoder to generate the desired text output. Concisely, the InstructBLIP output is represented as:

$$\omega_{insB} = l_d(l_e([\mathbf{t}_{qv}, p])) = l_d(l_e([Q(\mathbf{t}_q, v(i), p), p])). \quad (1)$$

**LLM (Decoder-only)** If instead of an encoder-decoder model, we consider a decoder-only model (add cite), we can treat the encoder to be an identity function i.e.  $l_e(\cdot, \cdot) = (\cdot, \cdot)$  and the output representation becomes:

$$\omega_{insB} = l_d(l_e([p, \mathbf{t}_{qv}])) = l_d([p, Q(\mathbf{t}_q, v(i), p)]). \quad (2)$$

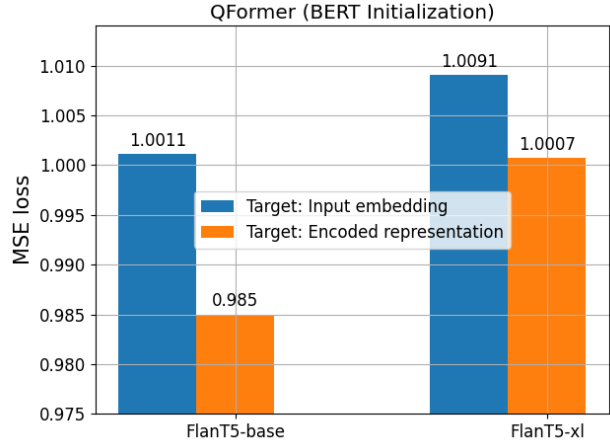


Figure 1. Experiment to study ease of modeling input embeddings vs encoder representations, the lower error indicates that the QFormer (BERT init) finds it easier to model the latter.

A key strength of the BLIP-2/InstructBLIP framework is that the image encoder  $v(\cdot)$ , the LLM encoder  $l_e(\cdot)$  (if present) and the LLM decoder  $l_d(\cdot)$  are frozen during training, with only the query tokens and the QFormer being trainable. Within the QFormer, the query tokens are allowed to interact with the prompt text tokens as well as each other via self-attention layers, and with the image features via alternate cross-attention blocks. The goal is to output a set of visually informed query tokens that can elicit an appropriate response from the downstream LLM encoder and decoder.

The QFormer [12] requires two heavy pretraining stages: Stage 1 comprises QFormer representation learning via image-text matching (ITM), image-text contrastive learning (ITC), and image-to-QFormer text generation (ITG) using the image encoder. Herein, the goal of the ITC and ITM is to align text features and query tokens in the QFormer latent space, whereas ITG trains the QFormer language modeling head for text generation by training the query tokens to extract visual features. Then, in Stage 2, these QFormer representations (“queries”) are projected onto the input space of the frozen LLM using a trainable fully-connected layer. These inputs are used to condition the frozen LLM for end-to-end image to text generation.

It is important to note that while in theory, Stage 1 pre-training requires more epochs, it only utilizes the frozen vision encoder and the QFormer model and is therefore a) requires less memory and b) LLM agnostic, since the same QFormer can be used as a plug-and-play model for different frozen LLMs, when initializing for Stage 2. On the other hand, pretraining in Stage 2 is LLM specific, which means adaptation to newer language models comes with additional computational burdens. Thus, we want to find a way to make this adaptation more efficient.

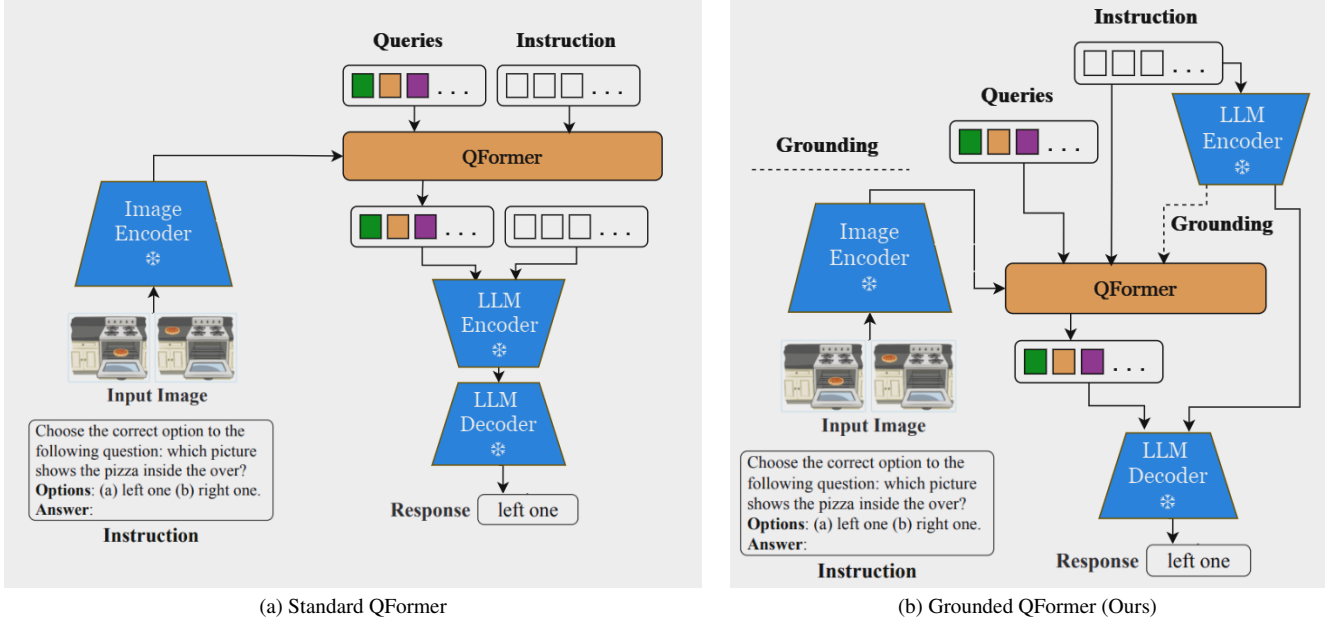


Figure 2. Illustration of our framework for vision language fusion with the language grounded QFormer (right), distinguishing it from the standard design (left) as proposed in InstructBLIP [5].

### 2.3. Analyzing QFormer Representations

Our first key observation stems from noting that the QFormer model is initialized as a language model, specifically a BERT encoder [6]. Thus while the outputs of the QFormer (the encodings) can be used to model language using language modelling heads, these encodings themselves are imbued with semantic meaning. And this holds not just for BERT encoders, but also for general encoder language models [18], wherein the encoder embeddings are often used for Sentence-level downstream tasks. However, note that in Stage 2, the QFormer latents are projected to the LLM input embedding space to condition vision-based generation. Thus, in essence, the standard QFormer tries to model the right syntactics for the frozen LLM, using representations based on the semantics of language.

It is accepted wisdom that the semantic essence of the data often lies on a lower-dimensional manifold, embedded in a higher-dimension (syntactic) input space [8]. For our application, we hypothesize that in terms of distributional similarity, the semantic latents of the QFormer correspond more strongly with the corresponding semantics of the LLM in the intermediate representations, as opposed to the LLM input text embeddings. Then, if the hypothesis holds, we could use the QFormer latents to directly model the LLM intermediates, to avoid this semantic-syntactic disparity in the standard QFormer pipeline and improve the learning efficiency of the framework.

To verify our hypothesis, we devise a simple experiment to compare the ease of modelling the LLM intermediates

to modelling the input embeddings, using the QFormer outputs. For this, we consider a representative subset of the Wikitext-103 dataset [17]. We consider the QFormer with default BERT initialization as in [5, 12], and for the LLM, two variants of the FlanT5 [3] family of encoder-decoder LLMs, flanT5-base (220M) and flanT5-xl (3B). The choice is for two reasons: a) ease of LLM intermediate extraction, since we know the encoder outputs are semantically meaningful and b) it is one of two family of models considered in the InstructBLIP work [5]. The experiment corresponds to a regression task; specifically, the same block of text is passed through the QFormer and the LLM. Then the outputs of the QFormer are projected via a linear projection (as in the standard framework) to match either the LLM input embeddings or the LLM encoder outputs, for the same text block via an L2 loss objective. For a fair comparison, we normalize both target distributions, input embeddings and encoder outputs, before training. The regression errors are reported in Fig. 1, which demonstrate that for both models, there is a noticeable drop in error when modelling the encoder representations, supporting our hypothesis.

### 2.4. Existing Alignment across Modalities

Additionally, the QFormer is designed to align representations across both language and vision modalities. Huh et al. [10] demonstrate that as vision models and language models scale up, their representational spaces converge across data modalities. Given that current deep learning models rely on hierarchical processing across layers, this motivates us

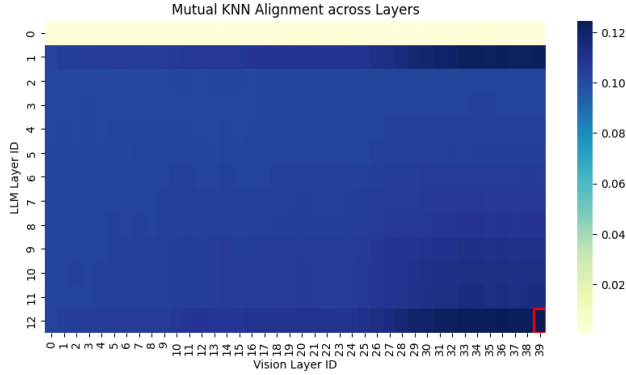


Figure 3. Mutual KNN alignment scores across the layers of an LLM (flanT5-base) and a vision transformer (Eva-clip-g/14) are presented as a heat map. The x-axis represents the layer IDs of the vision transformer, while the y-axis represents the layer IDs of the LLM. The maximum score is highlighted with a red box.

to ask a finer-grained question: Does the alignments across modalities vary across layers?

To explore this, we measure the existing alignment between the representations of a pre-trained language model, flanT5-base [3], and a pre-trained vision model, the CLIP-based vision transformer Eva-clip-g/14 [22], using the mutual KNN alignment metric proposed by Huh et al. [10]. Since flanT5-base employs an encoder-decoder architecture, our experiments focus on its encoder, emphasizing its representation learning capabilities.

For our measurements, we use the final token representation of the language model and the first token representation of the vision transformer, as these tokens are designed to aggregate the information from their respective inputs. Experiments were conducted on samples from COCO captioning validation set [2], with  $K=10$  neighbors, which has been shown to perform well in Huh et al. [10]. The computed alignment scores are averaged across samples for each layer, and the results are visualized in Figure 3.

The heat map reveals that higher alignment scores are achieved for deeper layers of both models, with the highest scores observed at their final layers. This may suggest that the common practice of aligning representations from a deeper layer of a vision model to the initial layer of a language model [12] might be suboptimal due to low alignment scores. Instead, aligning deeper layers with higher alignment scores could yield better results, as corroborated by our follow-up experiments in Section 3. This finding highlights the potential of using alignment to guide architecture design and further supports our hypothesis that aligning intermediate layers across modalities could enhance efficiency.

## 2.5. Grounding the QFormer

The observation in the previous sections is key to our method, in that, instead of directly feeding the LLM, the QFormer output tokens directly model a visually informed encoder latent representation, which is then fed to the LLM decoder for text image-to-text generation. To aid this process, we propose grounding these representations by augmenting the QFormer queries with representations of the input prompts from the LLM encoder. These representations act as a reference/feedback for modeling the encoder latent representation efficiently. Furthermore, we integrate the QFormer output directly into the LLM decoder, bypassing its encoder, due to the better cross-modal alignment demonstrated in Section 2.4.

We now provide a more precise characterization of our method, focusing on encoder-decoder LLMs. First, consider  $[\phi, p] = p$  as the concatenation of the prompt with an empty string, which serves as the input for the LLM encoder. Next, denote the language grounded QFormer as  $Q_g(\cdot, \cdot, \cdot)$  which accepts as input, language augmented queries ( $[t_q, l_e([\phi, p])]$ ), the image representations  $v(i)$  and the prompt  $p$ , to output grounded queries  $t_{qv-g} = Q_g([t_q, l_e([\phi, p])], v(i), p)$ . Then, InstructBLIP framework with the grounded QFormer ( $Q_g$ ) can be expressed as:

$$\begin{aligned} \omega_{g-insB} &= l_d([t_{qv-g}, l_e(p)]) \\ &= l_d([Q_g([t_q, l_e([\phi, p])], v(i), p), l_e([\phi, p])]). \end{aligned} \quad (3)$$

$$(4)$$

Note the two key differences from the standard QFormer (1), which is to use the encoded prompts as additional inputs to the QFormer. Second, QFormer output queries, along with the unaltered encoded prompts, are directly used to prompt language generation from the decoder. For better elucidation, we provide a visual comparison in Fig. 2.

We note that this grounding directly informs the QFormer of the encoder latent space; meaning that the QFormer obtains direct feedback while modelling the distribution of the latent representations that is expected, and can be suitably decoded by the LLM decoder. However, conditioning only the decoder leads to a natural tradeoff: the potential ease of modeling may be offset by the reduced model capacity to incorporate said conditioning, since the encoder is no longer involved in interpreting the QFormer queries. Our experiments show that benefits due to the former significantly outweigh the latter. Additionally, we find that splitting the LLM yields two other benefits: first, it reduces memory requirements for end-to-end training, as the encoder embeddings can now be precomputed. Second, inference/text generation is sped up significantly since decoding requires multiple forward passes through the entire LLM, whereas we only rely on the decoder.



Model	Captioning (BLEU-4)	VQA (Acc.) (%)
QFormer	0.238	57.72
Grounded (Ours)	<b>0.364</b>	<b>63.25</b>

Table 1. Performance comparison for single task models; each model is only trained on one task (either Captioning or VQA) and evaluated on the corresponding validation set.

### 3. Experiments

Here, we provide empirical evidence to support our hypothesis on more efficient training. Due to compute limitations, we restrict ourselves to smaller LLMs and datasets for our experiments. Specifically, we consider the FlanT5-base [3] as our frozen LLM and the Eva-clip-g/14 [22], a CLIP-based vision transformer, for the frozen image encoder.

Thus, it is important to point out that we do not intend to compete against the state-of-art InstructBLIP models. Indeed, it is not possible to replicate anymore since the LAION-5B dataset, the key component of QFormer pretraining, was taken offline due to questionable content [23]. Furthermore, it would require billion parameter LLMs and large scale pretraining, which we exclude from the scope of this work. Rather, in our small but controlled setup, we aim to compare the efficiency of the default QFormer pipeline against ours. Finally, for both frameworks, the QFormer uses the default architecture and initialization as in [5, 12], without any prior pretraining.

**Tasks** For this study, we primarily focus on two tasks: Captioning and Visual Question Answering (VQA). For captioning we consider the COCO captions dataset [2] and for visual question answering we consider VQAv2 [9] for training and OKVQA (Outside Knowledge VQA) [16] for zero-shot evaluation. To specify the task, we fix a set of text prompts for each task during training and randomly sample one prompt from that set for each iteration.

#### 3.1. Single Task Evaluation

We begin evaluating our grounded QFormer against the default one, without any pretraining, to establish baselines on captioning and question answering. Both models are trained under multiple hyperparameter configurations until training loss saturation, which takes about 50 epochs, and the respective best validation scores are reported. Our results in Table 1 indicate that our method significantly improves the learning capacity of the pipeline, even without any pretraining.

#### 3.2. Multi-task Training

A commonly sought advantage of VLMs is their ability to simultaneously perform different tasks well. To achieve such a model, pretraining followed by multi-task training/finetuning is effective [5, 12]. To emulate this, we train

multi-task models to perform both Captioning and VQA, by first using image captioning as the pre-training objective (20 epochs), and then performing multi-task instruction finetuning for captioning and VQA (15 combined epochs). The choice of our datasets, Coco Captions and VQAv2—which share same train-val-test image split—allows us to prevent train-test information leak for a fair evaluation. Note that this procedure also mimics pretraining with captioning, followed by an instruction finetuning procedure for training BLIP models. Results are given in Table 2. We find that for the designated scale pretraining followed by instruction finetuning task, our method achieves significant improvements over the standard QFormer. Additionally, we see that our method beats the single task baseline for VQAv2 (Table 1), harnessing the benefits of multi-task training and the synergy between captioning and VQA tasks.

#### 3.3. Zero-shot evaluation

Instruction finetuned VLMs can demonstrate remarkable zero-shot abilities and in the same vein, we evaluate the models on OKVQA, with results in Table 3. For comparison, we report the zero-shot OKVQA performance for BLIP-2 models [12] (InstructBLIP includes OKVQA during training, so comparison unavailable). Surprisingly, we find that our method demonstrates comparable zero-shot performance, despite utilizing two orders of magnitude less pretraining and much smaller LLMs.

#### 3.4. Pretraining Efficiency

Next, we compare the pretraining efficiency of both pipelines. Specifically, we evaluate the best validation score achieved for the captioning task within a fixed number of epochs, across different hyperparameter and learning rate configurations. Across all runs, we report the highest performance achieved within a fixed number of epochs. As shown in Fig. 4, we find that our method achieves significantly faster learning and better peak performance. Moreover, our modification to the original architecture allows the QFormer output to be integrated into an intermediate layer of the language model rather than the initial layer. This adjustment reduces computational overhead in the earlier layers, resulting in a training speed-up per epoch of 2.1%, as shown in Table 4. While this efficiency gain seems modest, it is due to our current reliance on the language encoder to provide inputs to the QFormer. However, in more recent VLM architectures with decoder-only LLMs, such as variants of LLaVA [14, 15], this computation is avoided. Consequently, we anticipate more significant training speedups in these newer architectures.

#### 3.5. Grounding Ablation

Finally, we study the effect of grounding i.e. feeding the encoded prompts to the QFormer. With the multi-task setup,

Model	Pretrain Captioning (BLEU-4)	Final Captioning (BLEU-4)	VQA (Accuracy) (%)
QFormer	0.231	0.209	55.4
Grounded (Ours)	<b>0.357</b>	<b>0.362</b>	<b>66.8</b>

Table 2. Performance comparison for pretraining, followed by multi-task instruction finetuning.

Model	OKVQA (Acc.) (%)	LLM
QFormer (Baseline)	28.83	FlanT5-base $\sim$ 240M
Grounded (Ours)	<b>38.96</b>	FlanT5-base $\sim$ 240M
BLIP-2 OPT	36.4	OPT $\sim$ 6.7B
BLIP-2 FlanT5-xl	40.7	FlanT5-xl $\sim$ 3B

Table 3. Zero-shot performance comparison on OKVQA.

Qformer	Ours
1.00	<b>0.979</b>

Table 4. Comparison of training times per epoch on the captioning dataset between the Qformer-based model and our model. The values are normalized relative to the Qformer-based model

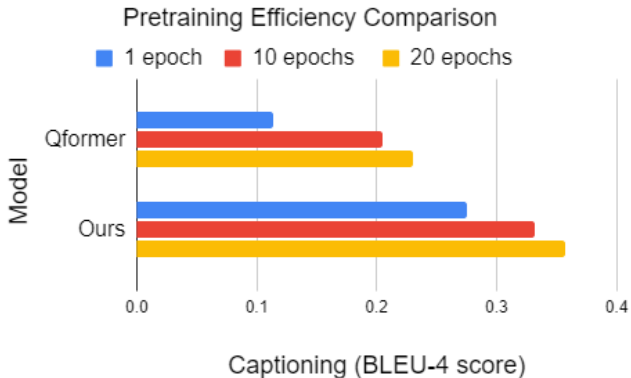


Figure 4. Pretraining comparison, showcasing our framework significantly improves pretraining efficiency.

we first pretrain two models, one with grounding and one without, to roughly the same captioning score, noting that the model without grounding takes an additional five epochs to reach similar performance. However, subsequent multi-task instruction fine-tuning reveals more pronounced advantages. Specifically, while the captioning score remains similar, we find that language grounding significantly speeds up VQA learning, with the grounded model maintaining a 5–6% performance lead in the earlier epochs and hitting peak performance much faster (see Fig. 5). This jives with our intuition that grounding aids the QFormer in learning the appropriate encoder latent representations for prompting the

Effect of Language Grounding on Multi-task learning

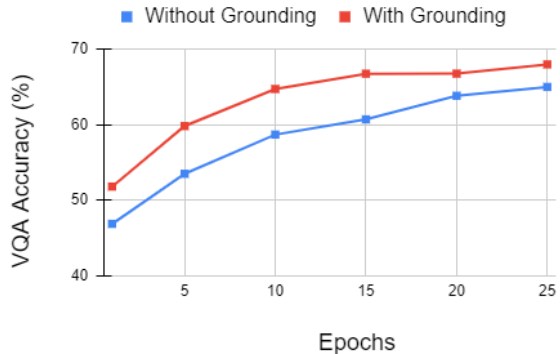


Figure 5. Grounding the QFormer with LLM encoder representations can significantly speed up multi-task learning, especially when the prompts are more informative of the task (as in VQA).

decoder, while noting that this speed-up is more significant for VQA, which incidentally generates more informative input prompts, i.e., image-based questions in this case.

#### 4. Towards a General Framework

Our experiments in the previous section show promise in terms of improving the efficiency of the standard QFormer pipeline. However, there are certain caveats. First, our experiments relied on encoder-decoder LLM architectures, whereas most modern state-of-the-art models rely on decoder-only architectures [19, 25]. Thus, although there is evidence to support decoder-only representations imbue semantics [20], it is unclear a) whether it can align with QFormer latents and b) what choice of intermediate layer representations is suitable for being modelled by the QFormer. Second, note that in our experiments, the QFormer is in its native BERT initialization. However, it is possible that after pretraining Stage 1, which involves joint vision-language training, the latents of the QFormer are affected such that our hypothesis about modelling the semantics vs. syntactics no longer holds. Even so, since the Stage 1 trained QFormer serves as a universal plug-and-play model, we would still like to utilize it when scaling up our framework. Therefore, we need to verify whether our hypothesis still holds.

For answering these questions comprehensively, we leave the more compute-intensive experiments for future

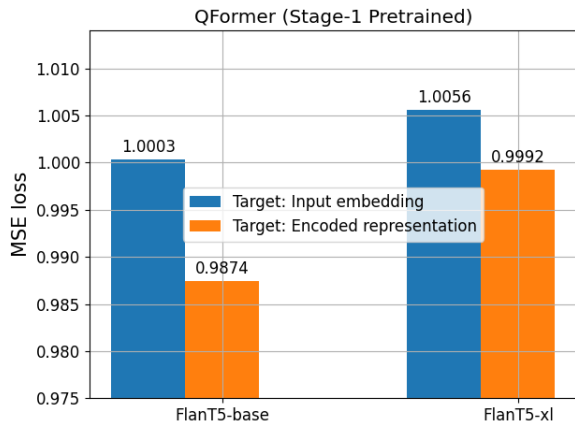


Figure 6. Experiment to study ease of modeling input embeddings vs encoder representations, the lower error indicates that the QFormer (Stage-1 pretrained) finds it easier to model the latter.

work. However, we offer some preliminary evidence by relying on our regression setup as before. Specifically, for the encoder-decoder models, we repeat the same experiment, but with the QFormer weights initialized from the pretraining Stage 1 checkpoint weights to check whether it changes the error trend. Fig. 6 again shows that even after pretraining, the QFormer representations are transferred to the encoder representations with more ease.

Next, to test our hypothesis for the decoder-only models, we consider the open-llama-3b-v2 [4, 7], an open source reproduction of llama-3b-v2 [25], consisting of twenty-four layers before the final decoding layer. To compare different intermediates, we consider a representative set of layers  $\{0, 8, 16, 24\}$ , where 0 refers to the input embeddings and for every other layer  $n$ , the regression targets are the outputs of the  $n^{th}$  layer. Since LLM outputs across layers can vary significantly in norm, we first normalize each target distribution to standard zero-mean and unit variance. The QFormer outputs are then projected using a linear layer to model the corresponding LLM representations. The respective errors are compared in Fig. 7, and we find that it is increasingly easier for the QFormer to model the LLM intermediates, the deeper we go into the network. Similar trends of increasing predictive power and clustering performance across layers within decoder-only models are observed by [28, 29].

## 5. Discussion & Future Work

In this work, we presented an alternative pipeline for QFormer-based vision-language fusion. We first showed that the QFormer latents are better suited to modelling the LLM intermediate outputs. Using this insight, we proposed our modified framework, which uses the QFormer to di-

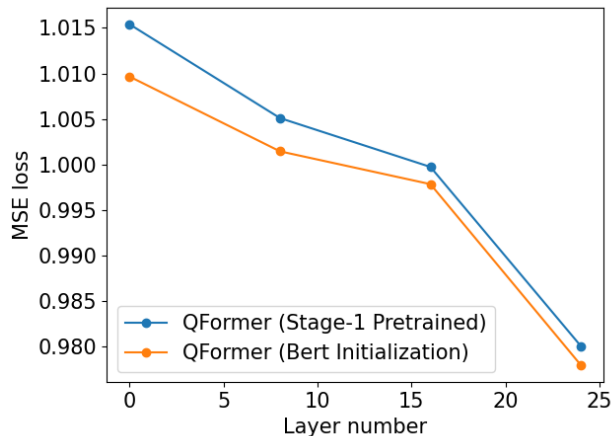


Figure 7. Experiment to study ease of modeling outputs from different layers of decoder-only LLM, open-llama-3b-v2. The results indicate that intermediate representations from deeper layers are easier to model, lending credence to our semantics hypothesis.

rectly condition generation in the LLM latent space, while also augmenting the pipeline with grounding for ease of latent modeling. Our experiments with encoder-decoder LLMs demonstrated an improvement in both performance and learning efficiency, when compared to the standard QFormer pipeline. Finally, we also highlighted potential for extending our method to decoder-only models.

However, there remains a performance gap to state-of-the-art models, arising from the limited LLM capacity and pretraining scale. Indeed, in our preliminary experiments with larger models, we observed performance dips for both methods when pretrained only on COCO captions ( $\sim 500k$  samples), indicating a need for scaling up pretraining, potentially to InstructBLIP levels ( $\sim 130m$  samples). A second limitation lies in the fact that extending our framework to decoder-only models may not be trivial; even though representation modelling may be easier in the intermediate layer, we also need enough depth in the model to be able to assimilate the visual information fed via the QFormer queries. We plan to explore this trade-off in future work by scaling up to: a) more pretraining and b) larger LLMs for better generative capabilities.

## References

- [1] Tom B. Brown, Benjamin Mann, Nick Ryder, Melanie Subbiah, Jared Kaplan, Prafulla Dhariwal, Arvind Neelakantan, Pranav Shyam, Girish Sastry, Amanda Askell, Sandhini Agarwal, Ariel Herbert-Voss, Gretchen Krueger, Tom Henighan, Rewon Child, Aditya Ramesh, Daniel M. Ziegler, Jeffrey Wu, Clemens Winter, Christopher Hesse, Mark Chen, Eric Sigler, Mateusz Litwin, Scott Gray, Benjamin Chess, Jack Clark, Christopher Berner, Sam McCandlish, Alec Radford, Ilya Sutskever, and Dario Amodei. Language models are few-shot learners. *CoRR*, abs/2005.14165, 2020. [1](#)
- [2] Xinlei Chen, Hao Fang, Tsung-Yi Lin, Ramakrishna Vedantam, Saurabh Gupta, Piotr Dollar, and C. Lawrence Zitnick. Microsoft coco captions: Data collection and evaluation server, 2015. [4](#), [5](#)
- [3] Hyung Won Chung, Le Hou, Shayne Longpre, Barret Zoph, Yi Tay, William Fedus, Yunxuan Li, Xuezhi Wang, Mostafa Dehghani, Siddhartha Brahma, Albert Webson, Shixiang Shane Gu, Zhuyun Dai, Mirac Suzgun, Xinyun Chen, Aakanksha Chowdhery, Alex Castro-Ros, Marie Pellat, Kevin Robinson, Dasha Valter, Sharan Narang, Gaurav Mishra, Adams Yu, Vincent Zhao, Yanping Huang, Andrew Dai, Hongkun Yu, Slav Petrov, Ed H. Chi, Jeff Dean, Jacob Devlin, Adam Roberts, Denny Zhou, Quoc V. Le, and Jason Wei. Scaling instruction-finetuned language models, 2022. [1](#), [2](#), [3](#), [4](#), [5](#)
- [4] Together Computer. Redpajama-data: An open source recipe to reproduce llama training dataset, 2023. [7](#)
- [5] Wenliang Dai, Junnan Li, Dongxu Li, Anthony Meng Huat Tiong, Junqi Zhao, Weisheng Wang, Boyang Li, Pascale Fung, and Steven Hoi. Instructblip: Towards general-purpose vision-language models with instruction tuning, 2023. [1](#), [2](#), [3](#), [5](#)
- [6] Jacob Devlin, Ming-Wei Chang, Kenton Lee, and Kristina Toutanova. Bert: Pre-training of deep bidirectional transformers for language understanding, 2019. [2](#), [3](#)
- [7] Xinyang Geng and Hao Liu. Openllama: An open reproduction of llama, 2023. [7](#)
- [8] Ian Goodfellow, Yoshua Bengio, and Aaron Courville. *Deep Learning*. MIT Press, 2016. [3](#)
- [9] Yash Goyal, Tejas Khot, Douglas Summers-Stay, Dhruv Batra, and Devi Parikh. Making the v in vqa matter: Elevating the role of image understanding in visual question answering, 2017. [5](#)
- [10] Minyoung Huh, Brian Cheung, Tongzhou Wang, and Phillip Isola. The platonic representation hypothesis. *arXiv preprint arXiv:2405.07987*, 2024. [3](#), [4](#)
- [11] Junnan Li, Dongxu Li, Caiming Xiong, and Steven Hoi. Blip: Bootstrapping language-image pre-training for unified vision-language understanding and generation, 2022. [2](#)
- [12] Junnan Li, Dongxu Li, Silvio Savarese, and Steven Hoi. Blip-2: Bootstrapping language-image pre-training with frozen image encoders and large language models, 2023. [1](#), [2](#), [3](#), [4](#), [5](#)
- [13] KunChang Li, Yinan He, Yi Wang, Yizhuo Li, Wenhai Wang, Ping Luo, Yali Wang, Limin Wang, and Yu Qiao. Videochat: Chat-centric video understanding, 2023. [1](#)
- [14] Haotian Liu, Chunyuan Li, Yuheng Li, and Yong Jae Lee. Improved baselines with visual instruction tuning. In *Proceedings of the IEEE/CVF Conference on Computer Vision and Pattern Recognition*, pages 26296–26306, 2024. [5](#)
- [15] Haotian Liu, Chunyuan Li, Qingyang Wu, and Yong Jae Lee. Visual instruction tuning. *Advances in neural information processing systems*, 36, 2024. [5](#)
- [16] Kenneth Marino, Mohammad Rastegari, Ali Farhadi, and Roozbeh Mottaghi. Ok-vqa: A visual question answering benchmark requiring external knowledge, 2019. [5](#)
- [17] Stephen Merity, Caiming Xiong, James Bradbury, and Richard Socher. Pointer sentinel mixture models, 2016. [3](#)
- [18] Jianmo Ni, Gustavo Hernández Ábrego, Noah Constant, Ji Ma, Keith B. Hall, Daniel Cer, and Yinfei Yang. Sentence-t5: Scalable sentence encoders from pre-trained text-to-text models. *CoRR*, abs/2108.08877, 2021. [3](#)
- [19] OpenAI, Josh Achiam, Steven Adler, Sandhini Agarwal, Lama Ahmad, Ilge Akkaya, Florencia Leoni Aleman, Diogo Almeida, Janko Altenschmidt, Sam Altman, Shyamal Anadkat, Red Avila, Igor Babuschkin, Suchir Balaji, Valerie Balcom, Paul Baltescu, Haiming Bao, Mohammad Bavarian, Jeff Belgum, Irwan Bello, Jake Berdine, Gabriel Bernadett-Shapiro, Christopher Berner, Lenny Bogdonoff, Oleg Boiko, Madelaine Boyd, Anna-Luisa Brakman, Greg Brockman, Tim Brooks, Miles Brundage, Kevin Button, Trevor Cai, Rosie Campbell, Andrew Cann, Brittany Carey, Chelsea Carlson, Rory Carmichael, Brooke Chan, Che Chang, Fotis Chantzis, Derek Chen, Sully Chen, Ruby Chen, Jason Chen, Mark Chen, Ben Chess, Chester Cho, Casey Chu, Hyung Won Chung, Dave Cummings, Jeremiah Currier, Yunxing Dai, Cory Decareaux, Thomas Degry, Noah Deutsch, Damien Deville, Arka Dhar, David Dohan, Steve Dowling, Sheila Dunning, Adrien Ecoffet, Atty Eleti, Tyna Eloundou, David Farhi, Liam Fedus, Niko Felix, Simón Posada Fishman, Justin Forte, Isabella Fulford, Leo Gao, Elie Georges, Christian Gibson, Vik Goel, Tarun Gogineni, Gabriel Goh, Rapha Gontijo-Lopes, Jonathan Gordon, Morgan Grafstein, Scott Gray, Ryan Greene, Joshua Gross, Shixiang Shane Gu, Yufei Guo, Chris Hallacy, Jesse Han, Jeff Harris, Yuchen He, Mike Heaton, Johannes Heidecke, Chris Hesse, Alan Hickey, Wade Hickey, Peter Hoeschele, Brandon Houghton, Kenny Hsu, Shengli Hu, Xin Hu, Joost Huizinga, Shantanu Jain, Shawn Jain, Joanne Jang, Angela Jiang, Roger Jiang, Haozhun Jin, Denny Jin, Shino Jomoto, Billie Jonn, Heewoo Jun, Tomer Kaftan, Łukasz Kaiser, Ali Kamali, Ingmar Kanitscheider, Nitish Shirish Keskar, Tabarak Khan, Logan Kilpatrick, Jong Wook Kim, Christina Kim, Yongjik Kim, Jan Hendrik Kirchner, Jamie Kiros, Matt Knight, Daniel Kokotajlo, Łukasz Kondraciuk, Andrew Kondrich, Aris Konstantinidis, Kyle Kosic, Gretchen Krueger, Vishal Kuo, Michael Lampe, Ikai Lan, Teddy Lee, Jan Leike, Jade Leung, Daniel Levy, Chak Ming Li, Rachel Lim, Molly Lin, Stephanie Lin, Mateusz Litwin, Theresa Lopez, Ryan Lowe, Patricia Lue, Anna Makanju, Kim Malfacini, Sam Manning, Todor Markov, Yaniv Markovski, Bianca Martin, Katie Mayer, Andrew Mayne, Bob McGrew, Scott Mayer McKinney, Christine McLeavey, Paul McMillan, Jake McNeil, David Medina, Aalok Mehta, Jacob



- Menick, Luke Metz, Andrey Mishchenko, Pamela Mishkin, Vinnie Monaco, Evan Morikawa, Daniel Mossing, Tong Mu, Mira Murati, Oleg Murk, David Mély, Ashvin Nair, Reichiro Nakano, Rajeev Nayak, Arvind Neelakantan, Richard Ngo, Hyeonwoo Noh, Long Ouyang, Cullen O’Keefe, Jakub Pachocki, Alex Paino, Joe Palermo, Ashley Pantuliano, Giambattista Parascandolo, Joel Parish, Emy Parparita, Alex Passos, Mikhail Pavlov, Andrew Peng, Adam Perelman, Filipe de Avila Belbute Peres, Michael Petrov, Henrique Ponde de Oliveira Pinto, Michael, Pokorny, Michelle Pocrass, Vitchyr H. Pong, Tolly Powell, Alethea Power, Boris Power, Elizabeth Proehl, Raul Puri, Alec Radford, Jack Rae, Aditya Ramesh, Cameron Raymond, Francis Real, Kendra Rimbach, Carl Ross, Bob Rotsted, Henri Roussez, Nick Ryder, Mario Saltarelli, Ted Sanders, Shibani Santurkar, Girish Sastry, Heather Schmidt, David Schnurr, John Schulman, Daniel Selsam, Kyla Sheppard, Toki Sherbakov, Jessica Shieh, Sarah Shoker, Pranav Shyam, Szymon Sidor, Eric Sigler, Maddie Simens, Jordan Sitkin, Katarina Slama, Ian Sohl, Benjamin Sokolowsky, Yang Song, Natalie Staudacher, Felipe Petroski Such, Natalie Summers, Ilya Sutskever, Jie Tang, Nikolas Tezak, Madeleine B. Thompson, Phil Tillet, Amin Tootoonchian, Elizabeth Tseng, Preston Tuggle, Nick Turley, Jerry Tworek, Juan Felipe Cerón Uribe, Andrea Valone, Arun Vijayvergiya, Chelsea Voss, Carroll Wainwright, Justin Jay Wang, Alvin Wang, Ben Wang, Jonathan Ward, Jason Wei, CJ Weinmann, Akila Welihinda, Peter Welinder, Jiayi Weng, Lilian Weng, Matt Wiethoff, Dave Willner, Clemens Winter, Samuel Wolrich, Hannah Wong, Lauren Workman, Sherwin Wu, Jeff Wu, Michael Wu, Kai Xiao, Tao Xu, Sarah Yoo, Kevin Yu, Qiming Yuan, Wojciech Zaremba, Rowan Zellers, Chong Zhang, Marvin Zhang, Shengjia Zhao, Tianhao Zheng, Juntang Zhuang, William Zhuk, and Barret Zoph. Gpt-4 technical report, 2024. [6](#)
- [20] Alec Radford, Jong Wook Kim, Chris Hallacy, Aditya Ramesh, Gabriel Goh, Sandhini Agarwal, Girish Sastry, Amanda Askell, Pamela Mishkin, Jack Clark, Gretchen Krueger, and Ilya Sutskever. Learning transferable visual models from natural language supervision. *CoRR*, abs/2103.00020, 2021. [6](#)
- [21] Emma Strubell, Ananya Ganesh, and Andrew McCallum. Energy and policy considerations for deep learning in NLP. *CoRR*, abs/1906.02243, 2019. [1](#)
- [22] Quan Sun, Yuxin Fang, Ledell Wu, Xinlong Wang, and Yue Cao. Eva-clip: Improved training techniques for clip at scale, 2023. [4](#), [5](#)
- [23] David Thiel. Identifying and Eliminating CSAM in Generative ML Training Data and Models. *Stanford Internet Observatory*, 2023. [5](#)
- [24] Julian Togelius and Georgios N. Yannakakis. Choose your weapon: Survival strategies for depressed ai academics, 2023. [1](#)
- [25] Hugo Touvron, Louis Martin, Kevin Stone, Peter Albert, Amjad Almahairi, Yasmine Babaei, Nikolay Bashlykov, Soumya Batra, Prajjwal Bhargava, Shrutí Bhosale, Dan Bikel, Lukas Blecher, Cristian Canton Ferrer, Moya Chen, Guillem Cucurull, David Esiobu, Jude Fernandes, Jeremy Fu, Wenyin Fu, Brian Fuller, Cynthia Gao, Vedanuj Goswami, Naman Goyal, Anthony Hartshorn, Saghar Hosseini, Rui Hou, Hakan Inan, Marcin Kardas, Viktor Kerkez, Madian Khabsa, Isabel Kloumann, Artem Korenev, Punit Singh Koura, Marie-Anne Lachaux, Thibaut Lavril, Jenya Lee, Diana Liskovich, Yinghai Lu, Yuning Mao, Xavier Martinet, Todor Mihaylov, Pushkar Mishra, Igor Molybog, Yixin Nie, Andrew Poulton, Jeremy Reizenstein, Rashi Rungta, Kalyan Saladi, Alan Schelten, Ruan Silva, Eric Michael Smith, Ranjan Subramanian, Xiaoqing Ellen Tan, Binh Tang, Ross Taylor, Adina Williams, Jian Xiang Kuan, Puxin Xu, Zheng Yan, Iliyan Zarov, Yuchen Zhang, Angela Fan, Melanie Kambadur, Sharan Narang, Aurelien Rodriguez, Robert Stojnic, Sergey Edunov, and Thomas Scialom. Llama 2: Open foundation and fine-tuned chat models, 2023. [6](#), [7](#)
- [26] Jason Wei, Maarten Bosma, Vincent Y. Zhao, Kelvin Guu, Adams Wei Yu, Brian Lester, Nan Du, Andrew M. Dai, and Quoc V. Le. Finetuned language models are zero-shot learners, 2022. [1](#)
- [27] Jason Wei, Xuezhi Wang, Dale Schuurmans, Maarten Bosma, Brian Ichter, Fei Xia, Ed Chi, Quoc Le, and Denny Zhou. Chain-of-thought prompting elicits reasoning in large language models, 2023. [1](#)
- [28] Xinbo Wu and Lav R Varshney. A meta-learning perspective on transformers for causal language modeling. *arXiv preprint arXiv:2310.05884*, 2023. [7](#)
- [29] Xinbo Wu and Lav R Varshney. Transformer-based causal language models perform clustering. *arXiv preprint arXiv:2402.12151*, 2024. [7](#)
- [30] Yi Zhang, Junyang Wang, and Jitao Sang. Counterfactually measuring and eliminating social bias in vision-language pre-training models. In *Proceedings of the 30th ACM International Conference on Multimedia*, page 4996–5004, New York, NY, USA, 2022. Association for Computing Machinery. [1](#)
- [31] Zijia Zhao, Longteng Guo, Tongtian Yue, Sihan Chen, Shuai Shao, Xinxin Zhu, Zehuan Yuan, and Jing Liu. Chatbridge: Bridging modalities with large language model as a language catalyst, 2023. [1](#)